Biochemical and Biophysical Research Communications 423 (2012) 110–115

Contents lists available at SciVerse ScienceDirect

Biochemical and Biophysical Research Communications

journal homepage: www.elsevier.com/locate/ybbrc

The inhibitory effect of BIM (I) on *L*-type Ca^{2+} channels in rat ventricular cells

Youn Kyoung Son [a,1], Da Hye Hong [a,1], Tae-Hoon Choi [b,1], Seong Woo Choi [c], Dong Hoon Shin [c], Sung Joon Kim [c], In Duk Jung [d], Yeong-Min Park [d], Won-Kyo Jung [e], Dae-Joong Kim [f], Il-Whan Choi [g,1], Won Sun Park [a,*,1]

[a] Department of Physiology, Kangwon National University School of Medicine, Chuncheon, Republic of Korea
[b] Department of Sport and Leisure Studies, Andong Science College, Andong, Republic of Korea
[c] Department of Physiology, Seoul National University College of Medicine, Seoul, Republic of Korea
[d] Department of Microbiology and Immunology and National Research Laboratory of Dendritic Cell Differentiation and Regulation, School of Medicine, Pusan National University, Yang-san, Republic of Korea
[e] Department of Marine Life Science, Chosun University, Gwangju, Republic of Korea
[f] Department of Anatomy and Cell Biology, Kangwon National University School of Medicine, Chuncheon, Republic of Korea
[g] Department of Microbiology, Inje University College of Medicine, Busan, Republic of Korea

ARTICLE INFO

Article history:
Received 15 May 2012
Available online 23 May 2012

Keywords:
BIM (I)
Protein kinase C
Ventricular myocytes

ABSTRACT

We investigated the effect of a specific protein kinase C (PKC) inhibitor, bisindolylmaleimide I [BIM (I)], on *L*-type Ca^{2+} channels in rat ventricular myocytes. BIM (I) alone inhibited the *L*-type Ca^{2+} current in a concentration-dependent manner, with a K_d value of 3.31 ± 0.25 μM, and a Hill coefficient of 2.34 ± 0.23. Inhibition was immediate after applying BIM (I) in the bath solution and then it partially washed out. The steady-state activation curve was not altered by applying 3 μM BIM (I), but the steady-state inactivation curve shifted to a more negative potential with a change in the slope factor. Other PKC inhibitors, PKC-IP and chelerythrine, showed no significant effects either on the *L*-type Ca^{2+} current or on the inhibitory effect of BIM (I) on the *L*-type Ca^{2+} current. The results suggest that the inhibitory effect of BIM (I) on the *L*-type Ca^{2+} current is independent of the PKC pathway. Thus, our results should be considered in studies using BIM (I) to inhibit PKC activity and ion channel modulation.

1. Introduction

L-type Ca^{2+} channels play an important role in regulating action potential duration, excitation–contraction (EC) coupling, and modulation of pacemaker activities in the cardiac muscle cells [1–3]. Indeed, a small influx of Ca^{2+} ions through *L*-type Ca^{2+} channels promotes Ca^{2+} release from intracellular Ca^{2+} storage. This process results in an increase in intracellular free Ca^{2+} concentration, which causes the EC coupling in the heart [4]. The changes in intracellular calcium concentration are one of the most important factors maintaining heart function; therefore, regulation of the Ca^{2+} channel is one of the main therapeutic targets for cardiovascular diseases, such as angina pectoris, hypertension, and certain cardiac arrhythmias [5,6].

Protein kinase C (PKC) is an important enzyme that plays a crucial role in many diverse cellular functions [7,8]. Biochemical and physiological studies have revealed that PKC activation is closely related to the release of hormones, cell growth, and generation of reactive oxygen species (ROS), cell cycle, differentiation, and modulation of ion channels [9–12]. Therefore, PKC inhibitors are indispensable tools for studies on PKC-related signaling mechanisms. To date, numerous PKC inhibitors have been developed and widely used in many laboratories. Among them, bisindolylmaleimide I [BIM (I)], which is a bis-indolemaleimide compound derived from staurosporine [13], inhibits the PKC ATP binding site with an IC_{50} value of 0.01 μM. Because BIM (I) shows higher selectivity for inhibiting PKC than that of staurosporine, BIM (I) is most widely and frequently used to inhibit PKC activity.

However, the unexpected effects of BIM (I) on other targets make it difficult to properly interpret experimental data. Thus, in the present study, we tested the effect of BIM (I) on *L*-type Ca^{2+} channels in freshly isolated rat ventricular myocytes with the expectation of supporting correct result interpretations in experiments related to Ca^{2+} dynamics.

2. Materials and methods

2.1. Cell preparation

Cells were prepared as described previously [14]. Briefly, male Sprague–Dawley rats (250–300 g) were anesthetized with a

* Corresponding author. Address: Department of Physiology, Kangwon National University School of Medicine, 1 Kangwondaehak-gil, Chuncheon 200-701, Republic of Korea. Fax: +82 33 255 8809.
E-mail address: parkws@kangwon.ac.kr (W.S. Park).
[1] These authors contributed equally to this work.

0006-291X/$ - see front matter © 2012 Elsevier Inc. All rights reserved.
http://dx.doi.org/10.1016/j.bbrc.2012.05.091

mixture of pentobarbital sodium (50 mg/kg) and heparin (300 U/ml). The procedure was conducted in accordance with the guidelines of the Committee for Animal Experiments of Kangwon National University. The heart was cannulated and then retrogradely perfused via the aorta on a Langendorff apparatus. After a 25–30 min collagenase (1 mg/10 ml, Yakult) enzymatic treatment, the left ventricle was dissected and agitated mechanically with a fire-polished Pasteur pipette to isolate single myocytes.

2.2. Electrophysiology

The *L*-type Ca^{2+} current was recorded in the whole-cell configuration using an Axopatch-1C amplifier (Axon Instruments Inc., Union, CA, USA), connected to a computer by a Digidata 1200 interface (Axon Instrument). Current was sampled at 2–4 kHz and filtered at 1–2 kHz.

2.3. Solution and drugs

The composition of normal Tyrode solution, and high-K^+ and low-Cl^- storage medium were described previously [14]. The bath solution for recording *L*-type Ca^{2+} current was (mM): 140 NaCl, 10 CsCl, 5 HEPES, 0.33 NaH_2PO_4, 0.5 $MgCl_2$, 16.6 glucose, 1.8 $CaCl_2$, titrated to pH 7.4 with NaOH. The pipette solution contained (mM); 106 CsCl, 20 TEA-Cl, 5 Mg-ATP, 5 NaCl, 10 HEPES, 10 EGTA, titrated to pH 7.25 with CsOH. BIM (I), iberiotoxin, paxilline, isoproterenol, and tetrodotoxin were purchased from Sigma Chemical Co. (St. Louis, MO). Rp-8-CPT-cAMPS and Rp-8-Br-PET-cGMPS were purchased from Biologic Life Science Institute (Bremen, Germany).

2.4. Data analysis

We used Origin 6.0 software (Microcal Software, Inc., Northampton, MA, USA) for data analysis. The kinetics of the interaction between the drugs and channel proteins is described based on a first-order blocking scheme [14,15]. The Hill equation was employed to calculate the apparent affinity constant (K_d), and the Hill coefficient was used for least-square fitting of the concentration dependent data:

$$f = 1/\{1 + (K_d/[D])^n\}$$

where f is fractional inhibition ($f = 1 - I_{drug}/I_{control}$) at each test potential, and $[D]$ is the drug concentration.

Steady-state activation was calculated from peak conductance:

$$G_{Ca} = I_{Ca}/(V_m - V_{rev})$$
$$d_{inf}(V) = G_{Ca}/G_{Ca,max}$$

where G_{Ca} is peak conductance, I_{Ca} is the peak Ca^{2+} current, V_m is the membrane voltage tested, $d_{inf}(V)$ is the steady-state activation parameter, and $G_{Ca,max}$ is the maximum value of G_{Ca}. V_{rev} represents reversal potential, which was measured as the zero-current potential in the *I–V* relationship.

The steady-state activation and inactivation curve data were obtained with individual two-pulse protocols, and fitted with the following Boltzmann equations, respectively:

$$y = 1/1 + \exp(-(V - V_{1/2})k) \text{ for activation;}$$
$$y = 1/1 + \exp((V - V_{1/2})k) \text{ for inactivation;}$$

where V is the test potential, $V_{1/2}$ is the voltage at half-maximum conductance, and k is the slope factor.

Data are presented as the mean ± SEM. The statistical analysis was performed with the Student's *t*-test. $P < 0.05$ was considered significant.

3. Results

3.1. BIM (I) inhibits the L-type Ca^{2+} channel in dose-dependent manner

For the recording of *L*-type Ca^{2+} channel, Cs^+ was included in the internal and external solutions to suppress the K^+ current. Tetrodotoxin (20 μM) was added to the bath solution, and the holding potential was maintained at −50 mV to block Na^+ and *T*-type Ca^{2+} current. Three μM BIM (I) inhibited the *L*-type Ca^{2+} current within 1 min throughout the whole voltage range tested (Fig. 1). Indeed,

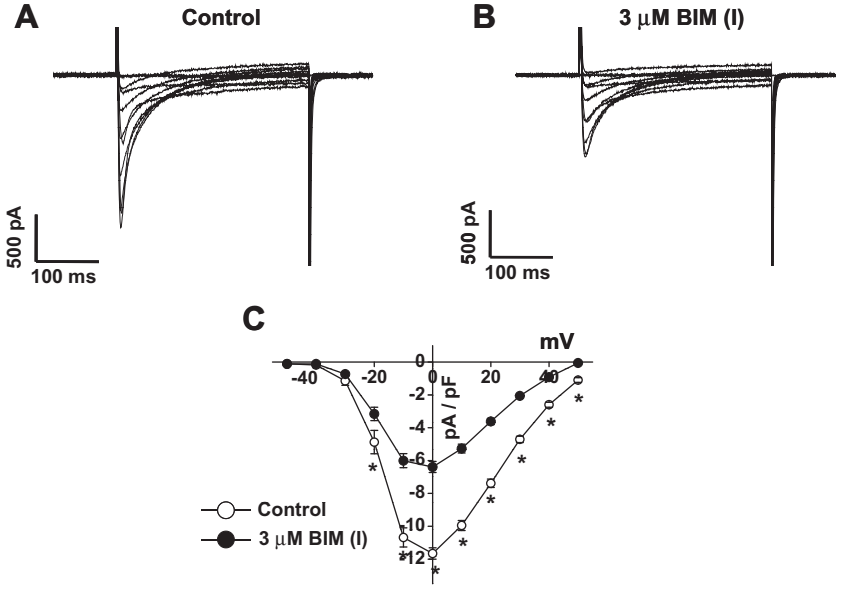

Fig. 1. The effect of BIM (I) on the *L*-type Ca^{2+} current. (A) Superimposed *L*-type Ca^{2+} current traces under the control condition recorded by 400-ms depolarization stimuli pulses in the voltage range of −50 ∼ + 50 mV from a holding potential of −50 mV. (B) Representative superimposed *L*-type Ca^{2+} current traces after applying 3 μM BIM (I), recorded using the same protocol as the control condition. (C) Summarized current–voltage (*I–V*) relationship from the peak Ca^{2+} current in the absence and presence of BIM (I) ($n = 8$). *$P < 0.05$.

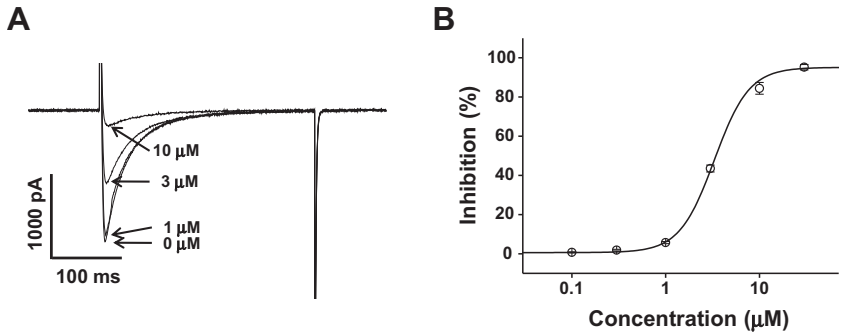

Fig. 2. BIM (I) inhibits *L*-type Ca^{2+} current in a dose-dependent manner. (A) Superimposed *L*-type Ca^{2+} current traces using a 400 ms depolarizing pulse of 0 mV from a holding potential of −50 mV, in the absence and presence of 1, 3, and 10 μM BIM (I). (B) Summary of percent inhibition for the peak current recorded at each concentration of BIM (I) ($n = 5$). Data were fit with the Hill equation.

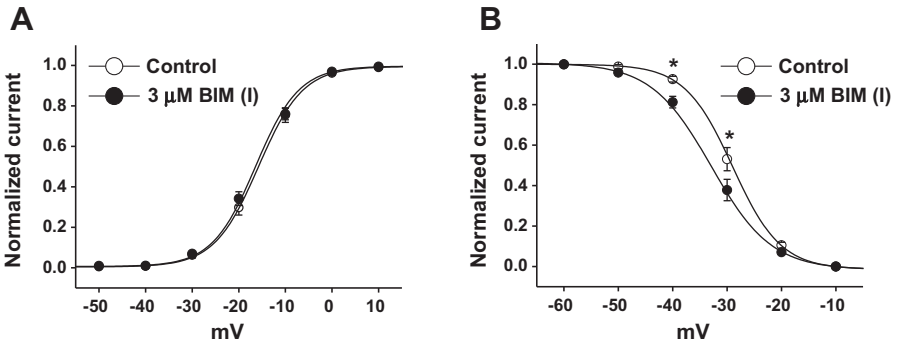

Fig. 3. Effects of BIM (I) on the voltage dependence of steady-state activation and inactivation of the *L*-type Ca^{2+} current. (A) Steady-state activation was determined from the peak conductance of each potential, in the absence and presence of BIM (I) ($n = 6$). (B) The steady-state inactivation curves were obtained from the peak current of a test pulse to 0 mV after a 2-s pre-pulse at each potential in the absence and presence of BIM (I) ($n = 4$). Data were fit with Boltzmann equation. $^{*}P < 0.05$.

the current density of *L*-type Ca^{2+} channel recorded at 0 mV was −11.66 ± 0.34 pA/pF under the control condition and −6.39 ± 0.34 pA/pF in the presence of 3 μM BIM (I) (Fig. 1C). These inhibitory reactions recovered to ~60% of the control condition after a 5 min washout (data not shown).

The inhibitory effect of BIM (I) on the *L*-type Ca^{2+} current was proportional to the BIM (I) concentration (Fig. 2). Current traces were recorded with depolarized pulses of 0 mV from a holding potential of -50 mV. The peak *L*-type Ca^{2+} current is summarized in Fig. 2B. Summarized data were fit with a non-linear least-square fitting of the Hill equation. The half maximum inhibition (K_d) was 3.31 ± 0.25 μM, and the Hill coefficient was 2.34 ± 0.23.

3.2. Effects of BIM (I) on steady-state activation and inactivation of the *L*-type Ca^{2+} channel

To investigate whether the inhibitory effects of BIM (I) affected the voltage dependence of the *L*-type Ca^{2+} channel, we analyzed the steady-state activation and inactivation of the *L*-type Ca^{2+} channel before and after applying BIM (I). For the activation curve, we applied a series of step-pulses through the voltage range of −50 to +10 mV, and the data were normalized by dividing the current amplitude by the electromotive force at each potential. The data obtained were least-square fitted with the Boltzmann equation (Fig. 3A). BIM (I) (3 μM) had no significant effects on voltage-dependent steady-state activation. The half-maximal activation ($V_{1/2}$) and the slope value (k) were −15.78 ± 0.37 and 4.75 ± 0.17 mV under the control condition, and −16.40 ± 1.08 and 4.65 ± 0.45 mV in the presence of 3 μM BIM (I).

BIM (I) (3 μM) shifted the inactivation curve to a negative potential for the voltage-dependence of the steady-state inactivation. The *L*-type Ca^{2+} channel inactivation curve was obtained using a double-pulse protocol: a 2-s pre-pulse for each potential and a test pulse of 0 mV for 300 ms. The peak test pulse current was measured and normalized to the maximum peak current, and fit with the Boltzmann equation (Fig. 3B). The half-maximal activation ($V_{1/2}$) and the slope value (k) were −28.98 ± 0.19 and 4.40 ± 0.10 mV in the control condition, and −32.92 ± 0.43 and 5.52 ± 0.22 mV in the presence of 3 μM BIM (I), respectively.

3.3. Other PKC inhibitors did not alter the inhibitory effect of BIM (I) on the *L*-type Ca^{2+} channel

We tested other PKC inhibitors on *L*-type Ca^{2+} channel to confirm whether the inhibitory effect of BIM (I) on the *L*-type Ca^{2+} channel was due to inhibiting PKC. As shown in Fig. 4, PKC inhibitory-peptide (PKC-IP), included in the pipette solution (dialyzed 10 min), did not affect the *L*-type Ca^{2+} current and did not significantly alter the inhibitory effects of BIM (I) on the *L*-type Ca^{2+} current. Addition of extracellular chelerythrine (3 μM, for 10 min), which is a general PKC inhibitor but structurally different from BIM (I), also did not affect the *L*-type Ca^{2+} current and did not significantly change the inhibitory effects of BIM (I) on the *L*-type Ca^{2+} current. These results strongly suggest that the inhibitory effect of BIM (I) on the *L*-type Ca^{2+} current was not due to inhibiting PKC.

4. Discussion

In this study, we investigated the effects of BIM (I) on the *L*-type Ca^{2+} channel in rat ventricular myocytes. BIM (I) (3 μM) decreased *L*-type Ca^{2+} channel activity within 1 min after the application, and

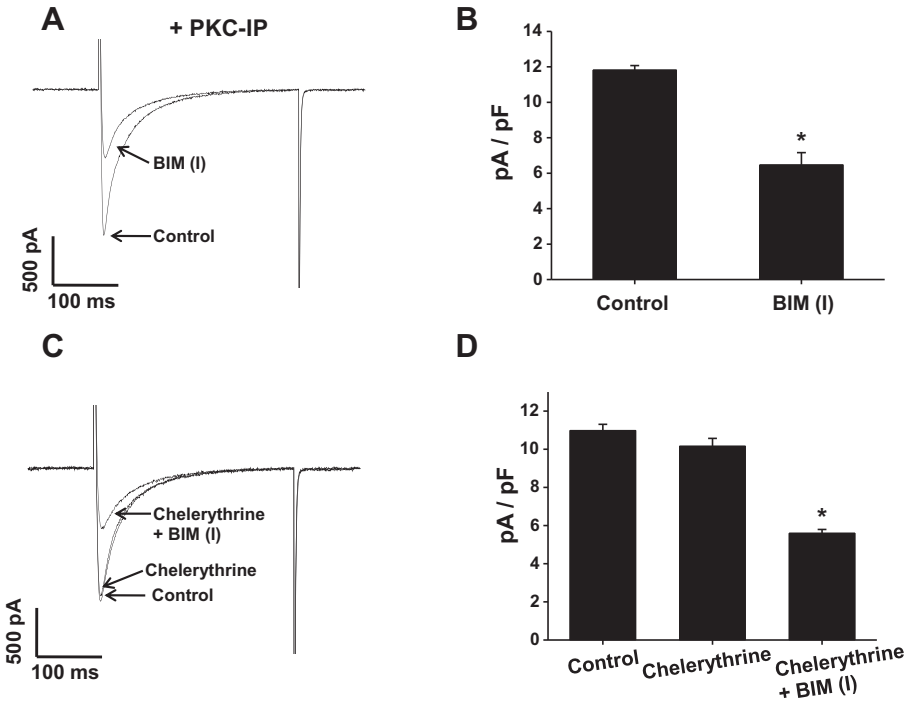

Fig. 4. Effects of other PKC inhibitors on the inhibition of the *L*-type Ca^{2+} current by BIM (I). (A) Representative *L*-type Ca^{2+} current traces were recorded in the absence and presence of BIM (I). 100 μM PKC-IP was included in the pipette solution. (B) Summary of the current densities preincubated with 100 μM PKC-IP in the absence and presence of BIM (I) ($n = 5$). (C) Representative *L*-type Ca^{2+} current traces were recorded using the same protocol as (A) under the control condition, in the presence of chelerythrine, and in the presence of chelerythrine together with BIM (I). (D) Summary of the current densities under the control condition, in the presence of chelerythrine, and in the presence of chelerythrine together with BIM (I) ($n = 4$) $^*P < 0.05$.

the inhibition was not voltage-dependent (Fig. 1) Additionally, the inhibitory effect of BIM (I) on the *L*-type Ca^{2+} channel was concentration-dependent (Fig. 2). BIM (I) did not significantly alter steady-state activation of the voltage-dependent *L*-type Ca^{2+} channel kinetics but shifted the steady-state inactivation curve toward a more negative potential, with changes in the slope factor of Boltzmann equation (Fig. 3).

The *L*-type Ca^{2+} channel plays a crucial role in cardiac function by regulating EC coupling, action potential duration, and intracellular Ca^{2+}-dependent signal transduction pathways [16,17]. Thus, controlling the *L*-type Ca^{2+} channel is important to maintain cardiac function. Because phosphorylation by protein kinases is the main regulatory mechanism for activating and/or inhibiting the *L*-type Ca^{2+} channel [18,19], several protein kinase inhibitors are widely used in studies on *L*-type Ca^{2+} channel-related signaling mechanisms.

However, several reports have proposed that protein kinase inhibitors have nonspecific actions toward untended targets. H-89, a protein kinase A (PKA) inhibitor, with an IC_{50} value of 0.048 μM [20], not only directly inhibits ATP-sensitive K+(K_{ATP}) channels (K_d = 1.19 μM), inward rectifier K^+ (Kir) channels (K_d = 3.78 μM), and voltage-dependent K+(Kv) channels (K_d = 1.02 μM) but also activates the big-conductance Ca^{2+}-activated K^+ (BK_{Ca}) channels (K_d = 0.47 μM) in coronary arterial smooth muscle cells [21–23]. Among PKC inhibitors, calphostin C (effective range, 0.05–0.25 μM [24]) inhibits *L*-type Ca^{2+} channels in ventricular myocytes at concentrations of 0.001–1 μM [25]. Another PKC inhibitor, chelerythrine (IC_{50} value for PKC = 0.7 μM [26]), inhibits acetylcholine-activated currents in PC12 cells at 0.1–10 μM, and atrial myocytes with an IC_{50} value of 0.49 μM [27]. Staurosporine (IC_{50} value for PKC = 0.0027 μM [28]), which has a similar structure to BIM (I), inhibits muscarinic K^+ channels in atrial myocytes in the concentration range of 10–100 μM, Kv1.3 channels expressed in CHO cells (IC_{50} = 1.2 μM), Kv channels in coronary arterial smooth muscle cells (IC_{50} = 1.3 μM), *L*-type Ca^{2+} channels in ventricular myocytes (IC_{50} = 0.062 μM), and Na^+ channels in ventricular myocytes (IC_{50} = 1.1 μM) [27]. Ro 31-8220 (IC_{50} value for PKC = 0.01 μM [29]) also directly inhibits Na^+ channels in cerebral cortex synaptosomes with an IC_{50} value of 1.1 μM [27], and Rottlerins specifically inhibits PKCδ (IC_{50} value for PKCδ = 3–6 μM [30]), directly activates BK_{Ca} channels expressed in HEK 293 cells at a concentration of 0.5 μM [27]. Additionally, U73122, a phospholipase C-specific inhibitor (IC_{50} = 0.2 μM [31]), inhibits BK_{Ca} channels (IC_{50} = 2.3 μM) and Kir3.1 channels (IC_{50} = 0.54 μM) expressed on HEK293 cells [32]. Genistein, a tyrosine kinase-specific inhibitor with an IC_{50} value of 0.002 μM [33] has many unexpected effects on ion channels. For example, genistein inhibits Kv4.3 (IC_{50} = 124.78 μM), hKv1.4 (50 μM used), and Kir2.3 (IC_{50} = 19.3 μM) channels expressed in CHO cells, Kir channels in rat osteoclasts (IC_{50} = 54 μM 5 min; 27 μM 10 min), delayed-rectifier K^+ channels in cardiac myocytes (IC_{50} = ~30 μM), Kv channels in coronary arterial smooth muscle cells (IC_{50} = 7.51 μM), T-type Ca^{2+} channels in spermatogenic cells (IC_{50} = 22.7 μM), and *L*-type Ca^{2+} channels in ventricular myocytes (IC_{50} = 17.5 μM) [34–41].

BIM (I) (IC_{50} value for PKC = 0.02 μM [13]) also showed side effects on ion channels. In fact, BIM (I) inhibits Kv1.5 channels expressed in CHO cells (IC_{50} = 0.38 μM), Kv channels in arterial smooth muscle cells (IC_{50} = 0.27 μM for rabbit coronary artery; 0.23 μM for rat mensenteric artery), Na^+ channels in cerebral cortex synaptosomes (IC_{50} = 10–100 μM), acetylcholine-activated K^+ channels in atrial myocytes (IC_{50} = 98.69 μM), and hERG channel expressed in *Xenopus* Oocytes (IC_{50} = 13.2 μM) [27,42–45]. However, to date, no studies have investigated the effects of BIM (I) on *L*-type Ca^{2+} channels. In this study, we showed that BIM (I) inhibited *L*-type Ca^{2+} channels with a K_d of 3.31 μM. As shown in Fig. 4, other PKC inhibitors, such as PKC-IP and chelerythrine, did

not affect the *L*-type Ca^{2+} current, and did not alter the inhibitory effect of BIM (I). Therefore, we conclude that the inhibitory effect of BIM (I) on the *L*-type Ca^{2+} channel seems independent of the PKC pathway.

The interaction mechanisms between *L*-type Ca^{2+} channels and its inhibitors have been suggested by previous reports [46–48]. Because BIM (I) and *L*-type Ca^{2+} channel inhibitors share structural similarities, predicting the interaction mechanisms between BIM (I) and the *L*-type Ca^{2+} channel is possible. The overall size of BIM (I) is similar to that of SQ 32910, a benzothiazepine based *L*-type Ca^{2+} channel inhibitor. Moreover, BIM (I) contains the functional groups (e.g., aromatic amines [such as puridine, purrole, and indole], carbonyl group, lots of amines, and aromatic rings), similar to the dihydropyridine based *L*-type Ca^{2+} channel inhibitors. These structural similarities between BIM (I) and the *L*-type Ca^{2+} channel inhibitors are found in drugs such as staurosporine, NS 1619, and BMS 204352, which also show inhibitory effects on the *L*-type Ca^{2+} channel besides their own function [14,27,49].

In the present study, we demonstrated that BIM (I) inhibited the *L*-type Ca^{2+} current in a concentration-dependent manner but independent of the PKC pathway. These results should be considered in studies when applying BIM (I) to regulate PKC in cells.

Acknowledgments

This research was supported by the National Research Foundation of Korea (NRF) Grant funded by the Korea government (MEST) (2010-0021126, 2011-0028573). Also, this study was supported by 2011 Research Grant from Kangwon National University.

Appendix A. Supplementary data

Supplementary data associated with this article can be found, in the online version, at http://dx.doi.org/10.1016/j.bbrc.2012.05.091.

References

[1] H. Irisawa, H.F. Brown, W. Giles, Cardiac pacemaking in the sinoatrial node, Physiol. Rev. 73 (1993) 197–227.
[2] S. Richard, F. Leclercq, S. Lemaire, C. Piot, J. Nargeot, Ca^{2+} currents in compensated hypertrophy and heart failure, Cardiovasc. Res. 37 (1998) 300–311.
[3] D.M. Bers, E. Perez-Reyes, Ca channels in cardiac myocytes: structure and function in Ca influx and intracellular Ca release, Cardiovasc. Res. 42 (1999) 339–360.
[4] A. Fabiato, Calcium-induced release of calcium from the cardiac sarcoplasmic reticulum, Am. J. Physiol. 245 (1983) 1–14.
[5] S. Yusuf, Calcium antagonists in coronary artery disease and hypertension: time for reevaluation?, Circulation 92 (1995) 1079–1082
[6] L.H. Opie, Pharmacological differences between calcium antagonists, Eur. Heart J. 18 (1997) 71–79.
[7] N. Divecha, R.F. Irvine, Phospholipid signaling, Cell 80 (1995) 269–278.
[8] Y. Nishizuka, Protein kinase C and lipid signaling for sustained cellular responses, FASEB J. 9 (1995) 484–496.
[9] M.A. Zamora, E.C. Dempsey, S.J. Walchak, T.J. Stelzner, BQ123, and ETA receptor antagonist, inhibits endothelin-1-mediated proliferation of human artery smooth muscle cells, Am. J. Respir. Cell Mol. Biol. 9 (1993) 429–433.
[10] A.C. Newton, Regulation of protein kinase C, Curr. Opin. Cell Biol. 9 (1997) 161–167.
[11] L.A. Shimoda, J.T. Sylvester, J.S. Sham, Inhibition of voltage-gated K^+ current in rat intrapulmonary arterial myocytes by endothelin-1, Am. J. Physiol. 274 (1998) 842–853.
[12] P.F. Li, C. Maasch, H. Haller, R. Dietz, R. von Harsdorf, Requirement for protein kinase C in reactive oxygen species-induced apoptosis of vascular smooth muscle cells, Circulation 100 (1999) 967–973.
[13] D. Toullec, P. Pianetti, H. Coste, P. Bellevergue, T. Grand-Perret, M. Ajakane, et al., The bisindolylmaleimide GF 109203X is a potent and selective inhibitor of protein kinase C, J. Biol. Chem. 266 (1991) 15771–15781.
[14] W.S. Park, S.H. Kang, Y.K. Son, N. Kim, J.H. Ko, H.K. Kim, et al., The mitochondrial Ca^{2+}-activated K^+ channel activator, NS 1619 inhibits L-type Ca^{2+} channels in rat ventricular myocytes, Biochem. Biophys. Res. Commun. 362 (2007) 31–36.
[15] D.J. Snyders, S.W. Yeola, Determinants of antiarrhythmic drug action. Electrostatic and hydrophobic components of block of the human cardiac hKv1.5 channel, Cir. Res. 77 (1995) 575–583.
[16] N. Frey, T.A. McKinsey, E.N. Olson, Decoding calcium signals involved in cardiac growth and function, Nat. Med. 6 (2000) 1221–1227.
[17] B. Fiedler, S.M. Lohmann, A. Smolenski, S. Linnemuller, B. Pieske, F. Schroder, et al., Inhibition of calcineurin-NFAT hypertrophy signaling by cGMP-dependent protein kinase type I in cardiac myocytes, Proc. Natl. Acad. Sci. USA 99 (2002) 11363–11368.
[18] H.C. Hartzell, Regulation of cardiac ion channels by catecholamines, acetylcholine and second messenger systems, Prog. Biophys. Mol. Biol. 52 (1988) 165–247.
[19] A.E. Lacerda, D. Rampe, A.M. Brown, Effects of protein kinase C activators on cardiac Ca^{2+} channels, Nature 335 (1988) 249–251.
[20] T. Chijiwa, A. Mishima, M. Hagiwara, M. Sano, K. Hayashi, T. Inoue, et al., Inhibition of forskolin-induced neurite outgrowth and protein phosphorylation by a newly synthesized selective inhibitor of cyclic AMP-dependent protein kinase, N-[2-(p-bromocinnamylamino)ethyl]-5-isoquinolinesulfonamide (H-89), of PC12D pheochromocytoma cells, J. Biol. Chem. 265 (1990) 5267–5272.
[21] Y.K. Son, W.S. Park, S.J. Kim, Y.E. Earm, N. Kim, J.B. Youm, et al., Direct inhibition of a PKA inhibitor, H-89 on K_V channels in rabbit coronary arterial smooth muscle cells, Biochem. Biophys. Res. Commun. 341 (2006) 931–937.
[22] W.S. Park, Y.K. Son, N. Kim, J.B. Youm, H. Joo, M. Warda, et al., The protein kinase A inhibitor, H-89, directly inhibits K_{ATP} and Kir channels in rabbit coronary arterial smooth muscle cells, Biochem. Biophys. Res. Commun. 340 (2006) 1104–1110.
[23] W.S. Park, Y.K. Son, N. Kim, J.B. Youm, M. Warda, J.H. Ko, et al., Direct modulation of Ca^{2+}-activated K^+ current by H-89 in rabbit coronary arterial smooth muscle cells, Vascul. Pharmacol. 46 (2007) 105–113.
[24] E. Kobayashi, K. Ando, H. Nakano, T. Iida, H. Ohno, M. Morimoto, et al., Calphostins (UCN-1028), novel and specific inhibitors of protein kinase C. I. Fermentation, isolation, physico-chemical properties and biological activities, J. Antibiot. (Tokyo) 42 (1989) 1470–1474.
[25] H.C. Hartzell, A. Rinderknecht, Calphostin C, a widely used protein kinase C inhibitor, directly and potently blocks L-type Ca channels, Am. J. Physiol. 270 (1996) 1293–1299.
[26] J.M. Herbert, J.M. Augereau, J. Gleye, J.P. Maffrand, Chelerythrine is a potent and specific inhibitor of protein kinase C, Biochem. Biophys. Res. Commun. 172 (1990) 993–999.
[27] Y.K. Son, D.H. Hong, D.J. Kim, A.L. Firth, W.S. Park, Direct effect of protein kinase C inhibitors on cardiovascular ion channels, BMB Rep. 44 (2011) 559–565.
[28] T. Tamaoki, H. Nomoto, I. Takahashi, Y. Kato, M. Morimoto, F. Tomita, Staurosporine, a potent inhibitor of phospholipid/Ca^{2+} dependent protein kinase, Biochem. Biophys. Res. Commun. 135 (1986) 397–402.
[29] C.T. Murphy, J. Westwick, Selective inhibition of protein kinase C. Effect on platelet-activating-factor-induced platelet functional responses, Biochem. J. 283 (1992) 159–164.
[30] C. Keenan, N. Goode, C. Pears, Isoform specificity of activators and inhibitors of protein kinase C γ and δ, FEBS Lett. 415 (1997) 101–108.
[31] C. Feisst, D. Albert, D. Steinhilber, O. Werz, The aminosteroid phospholipase C antagonist U-73122 (1-[6-[[17-β-3-methoxyestra-1,3,5(10)-trien-17-yl]amino]hexyl]-1H-pyrrole-2,5-dione) potently inhibits human 5-lipoxygenase in vivo and in vitro, Mol. Pharmacol. 67 (2005) 1751–1757.
[32] A. Klose, T. Huth, C. Alzheimer, 1-[6-[[17β-3-methoxyestra-1,3,5(10)-trien-17-yl]amino]hexyl]-1H-pyrrole-2,5-dione (U73122) selectively inhibits Kir3 and BK channels in phospholipase C-independent fashion, Mol. Pharmacol. 74 (2008) 1203–1214.
[33] T. Akiyama, J. Ishida, S. Nakagawa, H. Ogawara, S. Watanabe, N. Itoh, et al., Genistein, a specific inhibitor of tyrosine-specific protein kinases, J. Biol. Chem. 262 (1987) 5592–5595.
[34] H.J. Kim, H.S. Ahn, B.H. Choi, S.J. Hahn, Inhibition of Kv4.3 by genistein via a tyrosine phosphorylation-independent mechanism, Am. J. Physiol. Cell Physiol. 300 (2011) 567–575.
[35] Z.H. Zhang, Q. Wang, Modulation of a cloned human A-type voltage-gated potassium channel (hKv1.4) by the protein tyrosine kinase inhibitor genistein, Pflügers Arch. 440 (2000) 784–792.
[36] Z. Zhao, B. Liu, G. Zhang, Z. Jia, Q. Jia, X. Geng, et al., Molecular basis for genistein-induced inhibition of Kir2.3 currents, Pflügers Arch. 456 (2008) 413–423.
[37] F. Okamoto, K. Okabe, H. Kajiya, Genistein, a soybean isoflavone, inhibits inward rectifier K^+ channels in rat osteoclasts, Jpn. J. Physiol. 51 (2001) 501–509.
[38] T. Washizuka, M. Horie, K. Obayashi, S. Sasayama, Genistein inhibits slow component delayed-rectifier K currents via a tyrosine kinase-independent pathway, J. Mol. Cell Cardiol. 30 (1998) 2577–2590.
[39] E.A. Ko, W.S. Park, Y.K. Son, D.H. Kim, N. Kim, H.K. Kim, et al., The effect of tyrosine kinase inhibitor genistein on voltage-dependent K^+ channels in rabbit coronary arterial smooth muscle cells, Vascul. Pharmacol. 50 (2009) 51–56.
[40] J. Tao, Y. Zhang, S. Li, W. Sun, T.W. Soong, Tyrosine kinase-independent inhibition by genistein on spermatogenic T-type calcium channels attenuates mouse sperm motility and acrosome reaction, Cell Calcium 45 (2009) 133–143.

[41] C.E. Chiang, S.A. Chen, M.S. Chang, C.I. Lin, H.N. Luk, Genistein directly inhibits L-Type calcium currents but potentiates cAMP-dependent chloride currents in cardiomyocytes, Biochem. Biophys. Res. Commun. 223 (1996) 598–603.

[42] B.H. Choi, J.S. Choi, S.W. Jeong, S.J. Hahn, S.H. Yoon, Y.H. Jo, et al., Direct block by bisindolylmaleimide of rat Kv1.5 expressed in Chinese hamster ovary cells, J. Pharmacol. Exp. Ther. 293 (2000) 634–640.

[43] W.S. Park, Y.K. Son, E.A. Ko, J.H. Ko, H.A. Lee, K.S. Park, et al., The protein kinase C inhibitor, bisindolylmaleimide (I), inhibits voltage-dependent K^+ channels in coronary arterial smooth muscle cells, Life Sci. 77 (2005) 512–527.

[44] A. Kim, Y.M. Bae, J. Kim, B. Kim, W.K. Ho, Y.E. Earm, et al., Direct block by bisindolylmaleimide of the voltage-dependent K^+ currents of rat mesenteric arterial smooth muscle, Eur. J. Pharmacol. 483 (2004) 117–126.

[45] D. Thomas, B.C. Hammerling, A.B. Wimmer, K. Wu, E. Ficke, Y.A. Kuryshev, et al., Direct block of hERG potassium channels by the protein kinase C inhibitor bisindolylmaleimide I (GF109203X), Cardiovasc. Res. 64 (2004) 467–476.

[46] D.B. Tikhonov, B.S. Zhorov, Molecular modeling of benzothiazepine binding in the L-type calcium channel, J. Biol. Chem. 283 (2008) 17594–17604.

[47] D.B. Tikhonov, B.S. Zhorov, Structural model for dihydropyridine binding to L-type calcium channels, J. Biol. Chem. 284 (2009) 19006–19017.

[48] R.C. Cheng, D.B. Tikhonov, B.S. Zhorov, Structural model for phenylalkylamine binding to L-type calcium channels, J. Biol. Chem. 284 (2009) 28332–28342.

[49] Y.K. Son, S.W. Choi, W.K. Jung, S.H. Jo, I.D. Jung, Y.M. Park, et al., The inhibitory effect of Ca^{2+}-activated K^+ channel activator, BMS on L-type Ca^{2+} channels in rat ventricular myocytes, Life Sci. 89 (2011) 331–336.